Gas Permeability of Composite Membranes

JUIN-YIH LAI, *Department of Chemical Engineering, Chung Yuan University, Chung-Li, Taiwan 320, Republic of China,* SUMITO YAMADA, *Ashigara Laboratory, Fuji Film Co., Minami-Ashigara City, Kanagawa Prefat Japan,* KENJI KAMIDE, and SEI-ICHI MANABE, *Textile Research Lab., Asahi Chemical Industry Co., Takatsuki, Osaka, Japan,* TOHRU KAWAI, *Tanaka-Chiyo Women's College, 9, Minowa-cho, Machida-City, Tokyo, Japan*

Synopsis

The permeability of a composite membrane consisting of a homogeneous layer and a porous layer has been derived theoretically by assuming that the permeation through the homogeneous layer obeys Fick's law and that permeation through the porous layer is free molecular flow. The activation energy of the flow is described by three-dimensionless parameters, $\phi = |P_{12}/|P_2$, $\theta = d_1/d_2$, and $\sigma = |P_1/|P_2$. $|P_{12}$, $|P_1$, and $|P_2$ are the permeability coefficients of the composite membrane, the homogeneous layer and the porous layer, respectively, d_1 and d_2 are the thickness of the two layers. Once these parameters are determined, information on the structure of the membrane can be obtained (i.e., the pore size and the pore density). The permeabilities of various gases through homogeneous polycarbonate membrane, neutron-irradiated, nonsodium hydroxide-etched polycarbonate membrane, and their composite membrane were tested. A two-layer series model, incorporating the effect of neutron irradiation which produces some non-penetrating pores in the porous membrane layer, is proposed and agreed quite well with the experimental data.

INTRODUCTION

Gas separation by permeation through membranes has been suggested for many years.[1-4] Gas separation membranes may be divided into two categories: homogeneous dense and porous. For the efficient separation of gas mixtures, the membrane should have a high selectivity of a particular gas over other gases and also a high permeability to the gas. However, with homogeneous membranes high selectivity is usually associated with low permeability, as in the case of membranes used for oxygen enrichment from air.[5] On the other hand, porous membranes usually have very high permeabilities but their selectivity is generally quite low. The permeability of gases through porous polycarbonate membranes has been studied by Kamide, Kawai, and others.[6-10] Porous membrane with very small pores have some selectivity among various gases, but the selectivity is quite low compared to most homogeneous membranes.[10] Thus, composite membranes consisting of very thin active homogenes layers supported on a porous membrane with sufficient mechanical strength have been developed for many purposes. However, no theory exists that explains the permeability of gases through these composite membranes.

In this paper, the permeability of composite membranes consisting of a homogeneous active layer and porous polycarbonate membranes were studied both theoretically and experimentally.

Journal of Applied Polymer Science, Vol. 32, 4625–4637 (1986)
 CCC 0021-8995/86/044625-13$04.00

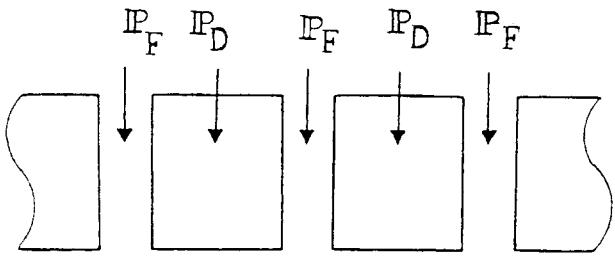

Fig. 1. Schematic representation of the parallel model.

THEORETICAL

In our model we assume that permeation through the homogeneous layer occurs by simple Fickian diffusion. Permeation through the porous support layer is assumed to occur by a combination of Fickian diffusion through the polymer matrix ($|P_D$) and free molecular flow through the pores ($|P_F$). We call this parallel flow. We will derive the equations for gas transport through the porous membrane by the parallel flow mechanism first, and then derive the expressions for the composite membranes. These two flow models are illustrated in Figures 1 and 2.

Parallel Model

Under the conditions mentioned above, the total permeation rate through the porous membrane can be formulated as:

$$Q = Q_F + Q_D \tag{1}$$

where Q is the total permeation rate, Q_F, the permeation rate by free molecular flow, and Q_D, the permeation rate by Fick's flow (cm^3/sc).

$$Q_D = DS(P_1 - P_2)/d \cdot \exp(-E/RT)(1 - \pi r^2 N) \tag{2}$$

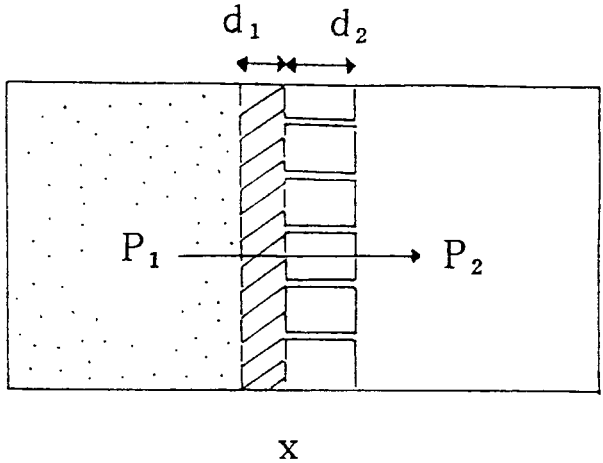

Fig. 2. Schematic representation of the composite membrane model composed of homogeneous and porous membranes.

where D = diffusion coefficient (cm^2/sc), S = solubility ($cm^3 gas/cm^3$ polymer), P_1 = pressure at higher pressure side (cm Hg), P_2 = pressure at lower pressure side, d = thickness of membrane (cm), E = diffusion activation energy (cal/mol), R = gas constant (cal/mole°K), T = temperature(°K), r = radius of pore (Å), N = pores/cm^2.

$$Q_F = 4/3 \cdot (2\pi RT/M)^{1/2} r^3/d \cdot (P_1 - P_2)(T_0/P_0T)N \tag{3}$$

where M = molecular weight of gas, P_0 = standard pressure, T_0 = standard temperature.

The relationship between permeability coefficient ($|P$) and permeation rate is: $|P = Q \cdot d/(P_1 - P_2)$.

Two-Layer Series Model

For the composite membrane which is composed of a homogeneous layer supported on a porous membrane, the series model as illustrated in Figure 2 applies. In Figure 2, P_1 and P_2 are again the pressures at the high and lower pressure sides, respectively, d_1 and d_2 are the thickness of the homogeneous and porous layers, respectively, and X respresents the position of the boundary between the two layers.

The permeation rate through the homogeneous membrane, Q_1 is:

$$Q_1 = DS(P_1 - P_x)/d_1 \exp(-E/RT) \tag{4}$$

where P_x is the pressure at the boundary between the two layers. As mentioned previously, the permeation rate, Q_2, through the porous layer in this case is shown by:

$$Q_2 = Q_F + Q_D \tag{5}$$

as in the case of (A), where

$$Q_F = 4/3 \cdot (2\pi RT/M)^{1/2} \cdot r^3/d_2 \cdot (P_x - P_2)T_0/P_0TN \tag{6}$$

$$Q_D = DS(P_x - P_2)/d_2 \cdot \exp(-E/RT)(1 - \pi r^2 N) \tag{7}$$

At steady state, $Q_1 = Q_2$. Therefore, using Eqs. (4)-(7), one can obtain P_x from the condition $Q_1 = Q_2$.

The permeability, $|P_{12}$, of the composite membrane can thus be obtained by:

$$|P_{12} = Q_1(d_1 + d_2)/(P_1 - P_2) \tag{8}$$

By using Norton's data of D, S, and E (13), the effect of porosity or radius on the permeability of helium gas through a polycarbonate homogeneous-porous composite membrane obeying the series model was calculated assuming $d_1 = d_2$, $N = 10^8$ and $T = 298.2$°K. The results are shown in Figure 3. The permeability coefficient increased with increasing radius or porosity in the range of 0 to 60 Å of radius. The leveling off at $r = 60$ Å means that the

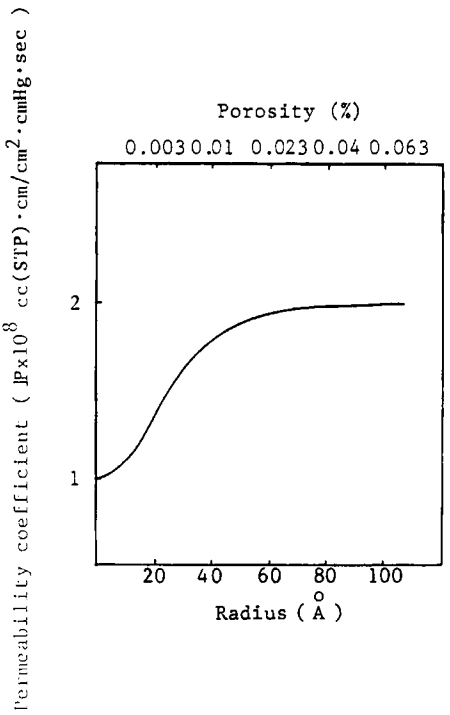

Fig. 3. Calculated dependence of gas permeability coefficient of porous polycarbonate composite membrane on pore radius. Gas: helium, $d_1 = d_2$, temp. = 298.2°K, N(pores/cm^2) = 10^8.

homogeneous membrane becomes rate controlling. Figure 4 shows the dependence of the permeability coefficient of helium through the polycarbonate composite membrane on temperature, calculated as a function of the density of pores or the porosity in the porous layer, assuming $d_2/d_1 = 50$ and $r =$ 20 Å. It can be seen that when the pore size is fixed and the density of the pore is small (i.e., $N = 10^8$ pores/cm^2) the plot of permeability vs. $1/T$ exhibits is linear and that the permeation behavior of the composite membrane is close to that of a simple homogeneous membrane since as little of the gas is permeated through the pores of the support membrane. On the other hand, the plot becomes nonlinear as the pore density increases, the apparent activation energy being dependent on T. It is interesting that the plot becomes linear again when the pore density increased to $N = 10^{12}$ where the homogeneous top layer membrane became rate controlling.

Figure 5 shows the dependence of the permeability coefficient of helium through the composite membrane on temperature, calculated as a function of pore size, assuming $d_2/d_1 = 25$ and $N = 10^8$ pores/cm^2. It can be seen that if the pore density is fixed, the relationship of permeability vs. $1/T$ is linear for small pore size, nonlinear for larger size, and linear again for much larger pores.

From the results of these calculation, it is apparent that we can estimate the structure of the membrane, in terms of the ratio of thickness of the two layers, the pore size, and the pore density by measuring the temperature dependency of the membrane permeability.

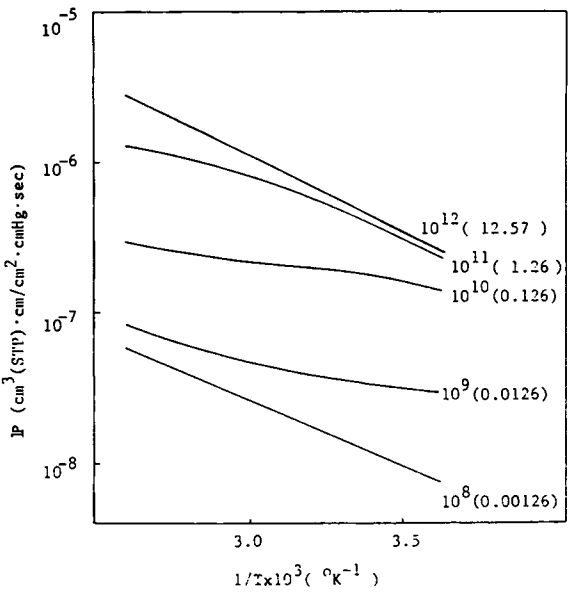

Fig. 4. Calculated temperature dependence of gas permeability coefficient of porous polycarbonate composite membrane. Gas: helium, $d_2/d_1 = 50$, $r = 20$ Å. The density of pores N(pores/cm^2) and the porosity (%) in the parentheses are shown on each curve.

For this purpose, another approach has been made based on a simple equation on the general composite membrane (14):

$$d_1 + d_2/|P_{12} = d_1/|P_1 + d_2/|P_2 \tag{9}$$

This may be rewritten:

$$|P_{12}/|P_2 = (d_1/d_2 + 1)/(|P_2 d_1/|P_1 d_2 + 1) \tag{10}$$

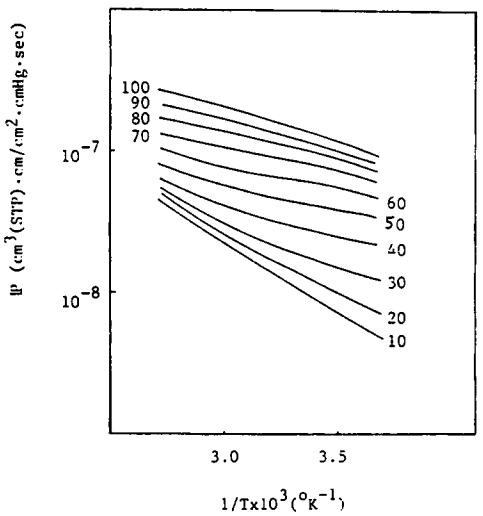

Fig. 5. Calculated temperature dependence of gas permeability coefficient of polycarbonate composite membrane. Gas: helium, $d_2/d_1 = 25$, $N = 10^8$ pores/cm^2, the r value in Å are shown on each curve.

Let

$$\phi = |P_{12}/|P_2, \qquad \theta = d_1/d_2, \qquad \text{and} \qquad \sigma = |P_1/|P_2$$

we obtain:

$$\phi = (\theta + 1)/(\theta/\sigma + 1) \tag{11}$$

By changing θ, the pore size r, the pore density N, and temperature T, the activation energy was calculated by our theory as a function of the three-dimensionless parameters ϕ, σ, and θ. The results are shown in Figure 6. The dotted curves show equiactivation energy which obviously reflects Figures 4 and 5. It can be seen that the range of the change in the activation energy decreases as θ is increased. As ϕ increases up to 10, it is seen that the permeation of the homogeneous layer becomes rate controlling. As $\phi = \sigma = 0$, this is the case when the pore size of the porous layer is very small and the composite membrane can be treated as a simple homogeneous membrane. In the case of $\phi = \sigma = 1$, the homogeneous layer is again rate controlling, since the permeability through the porous layer is much larger than that of the homogeneous layer.

Once such three-dimensional plots were made for a particular material of the membrane and a gas, the above parameters representing the structure of the membrane can be obtained by measuring the activation energy of the permeation. When θ is known, and the activation energy of the permeation is measured, we can determine ϕ and σ from Figure 6. This implies that we now know $|P_1$ and $|P_2$, since $|P_{12}$ was measured. Since all the quantities in Eqs. (4), (6), and (7) are known except r and N, we can obtain r and N by simple iteration.

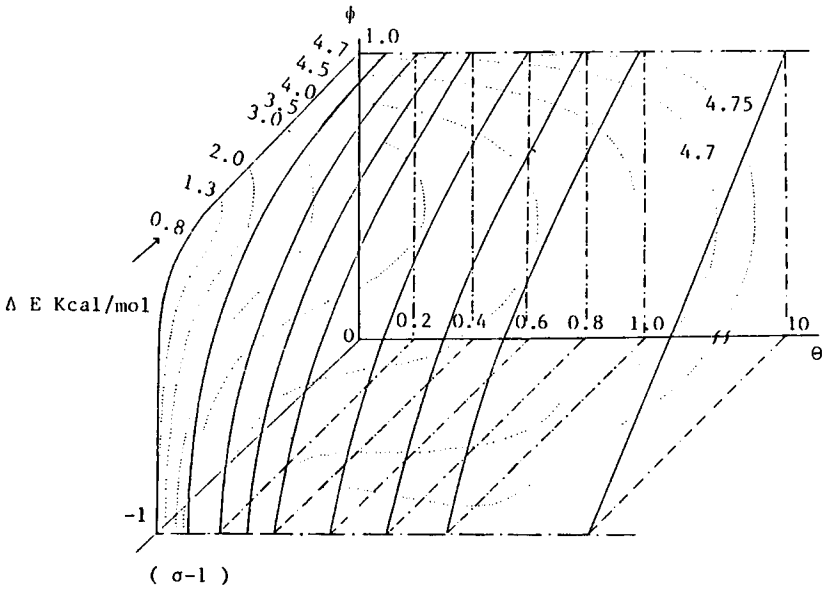

Fig. 6. Calculated three dimensional plot of the activation energy as a function of the parameter, ϕ, θ, σ.

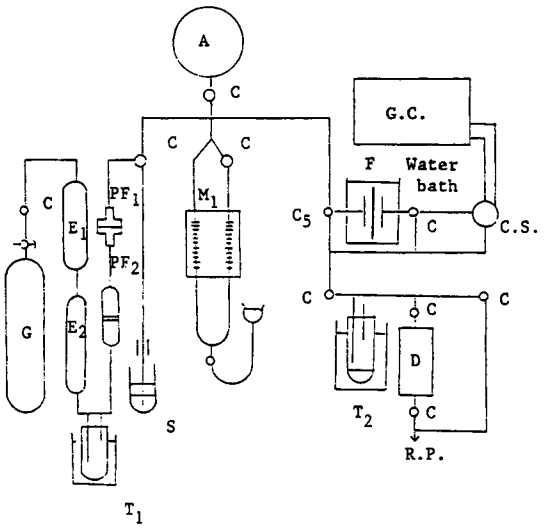

Fig. 7. Schematic representation of the instrument measuring gas permeability coefficient: G; a gas reservior, E_1 and E_2; the tubes for drying the gas containing calcium chloride and phosphorous pentoxide, respectively, PF_1 and PF_2; prefilters of Nuclupore (Nu 0.015) membrane of G.E. Co. and of porous ceramics, respectively, A; the reservoir of the gas at the higher pressure side, M_1; manometer, T_1 and T_2; trap tubes, D; diffusion pump, F; the cell divided into the two parts by the membrane, C and C.S.; rotational cocks, G. C.; gas chromatograph.

EXPERIMENTAL

1. Gases. Helium, oxygen, and nitrogen of 99.9% purity were used.

2. Apparatus. The apparatus for measuring the permeability of the gas is shown in Figure 7.

3. Measurement of Gas Permeability. The volume of the vessel at the higher pressure side is 3 ℓ, and that at lower pressure side is 4.7 cm^3. No change was made in the higher pressure side during the test. The concentration of gas on the permeate side of the membrane was measured by gas chromatography. By the calibration for each gas, we obtained dP_2/dt and the permeability coefficient $|P$ was calculated by the following equation:

$$|P = (T_0 dV/TP_0A) \cdot (1/P_1 - \Delta P_2) \cdot (dP_2/dt) \tag{12}$$

where A = area of the membrane, V = volume at lower pressure side, ΔP_2 = pressure change at lower pressure side, T_0 = the standard temperature (273.2°K), and P_0 = the standard pressure (76 cm Hg).

4. Preparation and Characterization of Membranes. Polycarbonate membrane made by the G.E. Co. was coated by polyvinylpyrrolidone (PVP) and paraffin used for packing purposes. After PVP and paraffin were washed out, the homogeneous membrane was dissolved in chloroform and then case onto mercury and the solvent is evaporated to form the homogeneous membrane for this study. Using electron microscopy, the homogeneous membranes prepared were confirmed to have no pin hole.

The Nucleopore membranes of G.E. Co. were made by neutron irradiating the homogeneous membrane mentioned above and then by etching the pores

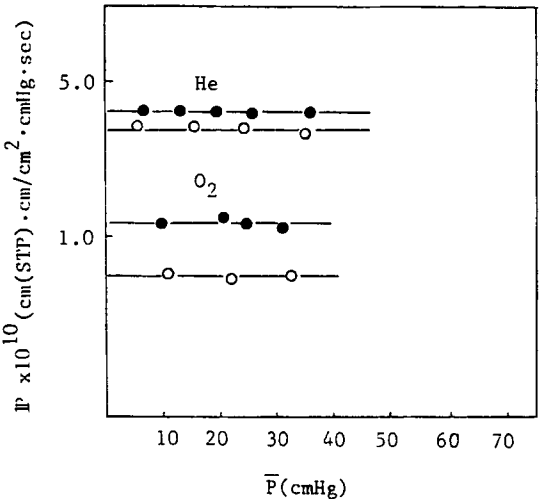

Fig. 8. Mean pressure $\bar{P}$ dependence of gas permeability coefficient $|P$ of the homogeneous and irradiated porous membranes. ○: homogeneous membrane, ●: irradiated porous membrane temperature: 293.2°K.

of the membrane by 6N NaOH. To form membranes with very small pore size, the membranes without NaOH etching were specially supplied by G.E. Co. These membranes were also washed by *n*-hexane and methanol successively to remove PVP and paraffin. The pores in these membranes were so small that they could not be detected by electron microscopy, at magnifications of up to 100,000.

The thickness of the membrane measured from the absorption of visible light as a function of wavelength, was from 0.70 to 2.34 μm for the homogeneous membranes and 12.87 μm for the porous membranes. The above two types of membranes were simply attached and the exterior of the permeating area was bonded by using an adhesive agent.

RESULTS AND DISCUSSION

Figure 8 shows the dependence of the permeability coefficient of the homogeneous membrane on the mean pressure, $\bar{P}$ of $|P_1$ and $|P_2$. It is seen that the permeability does not depend on the mean pressure, implying that no pin hole exists in the membrane. The permeability coefficients of He and O_2 through the irradiated porous membrane are also shown in Figure 8. It indicates that the viscous flow theory cannot be applied and the free molecular flow and Fick's flow assumed in the present theory holds for the porous membrane. From the observation under an electron-microscope mentioned before, we can assume that there are no pores with sizes more than 100 Å. The mean free path was calculated for the maximum and minimum pressures of the gases used and is shown in Table I. For all the gases used, the mean free path, λ is much larger than the pore size of 100 Å. Therefore, it is reasonable to say that free molecular flow is present in this porous membrane.

Figure 9 shows the permeability coefficient $|P$ of the various gases through the irradiated porous membrane plotted against $1/T$. Figure 10 includes the

TABLE I
Mean Free Path of Gases at Maximum and Minimum Pressures Used

gas	P_{max}[a]	P_{min}[a]	max[b]	min[b]
H_2	72.11	12.14	76.16	12.82
He	71.51	12.05	117.24	19.76
O_2	72.52	11.72	45.19	7.30
N_2	73.18	12.52	112.34	6.53
CO	71.70	12.24	39.44	6.73
CO_2	71.77	11.89	27.03	4.48
Ar	71.92	12.15	42.77	7.23

[a] cm Hg.
[b] $\times 10^6$ cm.

temperature dependency of the permeability coefficient of the homogeneous membranes. The activation energy and the permeability extraporated to $1/T = 0$ obtained from these data for the homogeneous membranes are shown in Table II. From Figures 9 and 10, it can be seen that (a) The permeability of the irradiated porous membrane is higher than that of the homogeneous membrane. (b) The activation energy is lower for the irradiated porous membrane than that for the homogeneous membrane. (c) The permeability through the irradiated porous membrane does not depend on the molecular weight of the gas.

From the results of (a) and (b), it can be concluded that Fick's law cannot be applied to the irradiated porous membrane. The free molecular flow cannot be applied because of the result (c). Moreover, the permeability should be proportional to $T^{1/2}$ for the free molecular flow. Therefore, the parallel model mentioned above is likely to be able to apply to the irradiated porous membranes.

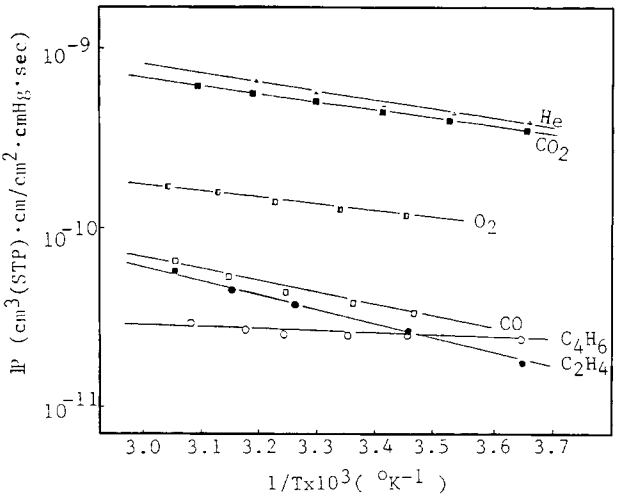

Fig. 9. Temperature $1/T$ dependence of gas permeability coefficient $\bar{P}$ of the irradiated porous membrane (not chemical etched).

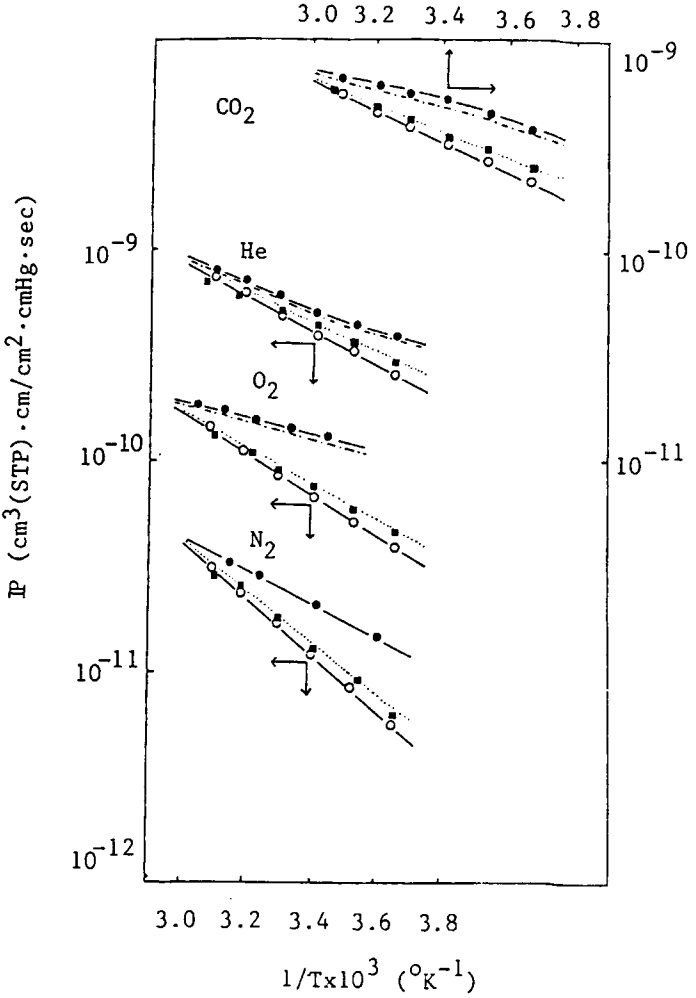

Fig. 10. Comparison of the theory based on the two-layer series models with the observed values of gas permeability coefficient as a function of temperature for the homogeneous and irradiated porous membranes and their composite membrane. (The irradiated membrane side was exposed to higher pressure.) —·—: the parallel model for the irradiated porous membrane; ----------: the series model for the irradiated porous membrane; ○: observed values of homogeneous membrane; ●: observed values of irradiated membrane; ■: observed values of composite membrane; d_1 (irradiated porous layer) = 12.87 μm, and d_2 (homogeneous layer) = 1.46 μm.

TABLE II
Activation Energy and Permeability Coefficient Extraporated to $1/T = 0$ in the Homogeneous Polycarbonate Membrane

	E(kcal/mol)	$P_0 \times 10^7$
He	4.09	1.27
O_2	4.24	8.67
N_2	5.96	—
CO_2	3.25	9.50

Then, for the irradiated porous membrane, we can write from Eqs. (1) to (3):

$$|P = 1.09 \times 10^5 r^3 N(1/MT)^{1/2} + (1 - \pi r^2 N)|P_D \tag{13}$$

where $|P_D$ is the permeability coefficient corresponding to Q_D. Since $r <$ 100 Å, and $N_{\max} \leqq 10^9$, $\pi r^2 N \leqq 3 \times 10^{-3}$, and $1 - \pi r^2 N \simeq 1$ for He, at 25°C. Thus,

$$|P = 3.17 \times 10^3 r^3 N + |P_D \tag{14}$$

This shows that the difference in the permeability coefficient between the porous membrane and the homogeneous membrane should be $3.17 \times 10^3 r^3 N$.

The density of pores N of the G.E. Nucleopore membrane is in the range of 1.6×10^7 to $1.0 \times 10^9/\text{cm}^2$. The radius of the pores obtained from Eq. (14), using the data in Table II for the homogeneous membrane as $|P_D$, are thus in the range of 3.05 Å to 12.11 Å, which cannot be detected by electron microscopy. Using the value of r^3N obtained above, we can calculate the permeability coefficient of helium as a function of T by Eq. (14) with the data in Table II. The result is shown in Figure 11. The dotted curve (with 2.3 mark) was calculated by Eq. (14) assuming $\Delta E = 2.3$ Kcal/mol, which coincides with the observed activation energy at 20°C. Another dotted curve (marked 3.7) was calculated by Eq. (14) so that the permeability at 20°C coincides with the observed figure. The calculated results do not agree with the observed curve. Therefore, the two-layer series model was applied to this particular irradiated porous membrane. Assuming $N = 8 \times 10^7$, $r = 18$ Å, d_1 (porous layer) = 12.12 μm, and d_2 (homogeneous layer) = 0.75 μm, good agreement with the experimental data was obtained as shown in Figure 11. Figure 10 shows the comparison of the theory based on the two-layer series

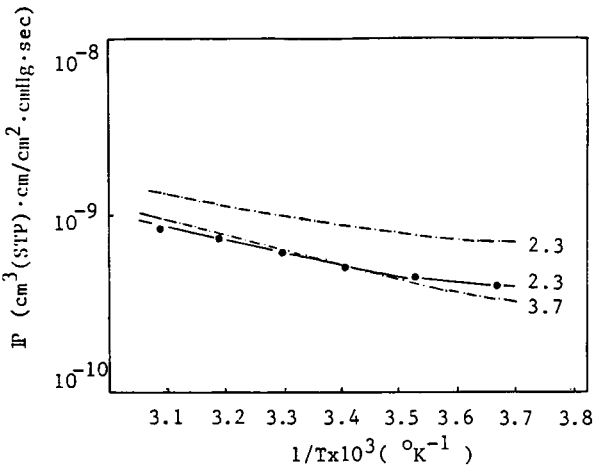

Fig. 11. Calculated and observed temperature dependence of permeability coefficients of helium for the irradiated porous membrane. — - — - —: straight porous structure was assumed; —: the series model with $d_1 = 12.12$ μm and $d_2 = 0.75$ μm was assumed; ●: observed values. The number on each curve represents the activation energy (kcal/mole) assumed.

model for the composite membrane, in which the parallel and series models were applied to the irradiated porous membrane, with the experimental data. It can be seen that quite a good agreement between the theory and experimental data was obtained when the two-layer series model was used for the irradiated porous membrane, but not when the parallel model was used for the irradiated porous membrane. Applying the series model for the composite membrane consisting of a homogeneous membrane and the irradiated porous membrane which obeys again the two-layer series model, the experimental data could be completely explained.

Finally, it is of interest to note that a difference in permeability was observed when the flow of gas is from the opposite direction. The result of Figure 10 was obtained when the irradiated membrane side was exposed to the

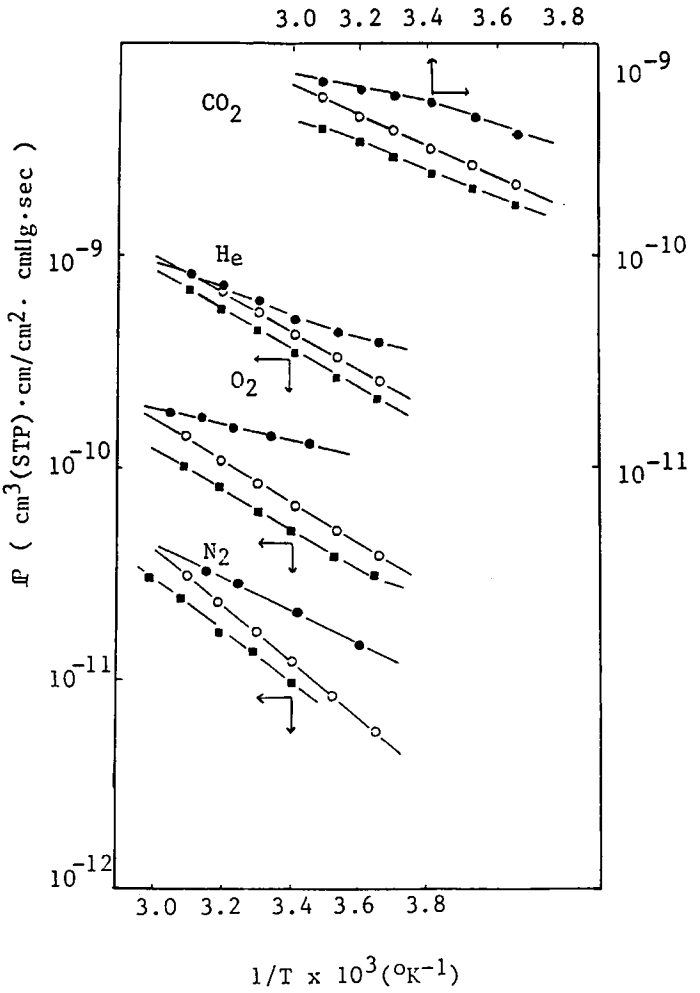

Fig. 12. Comparison of the observed values of gas permeability coefficient as a function of temperature for the homogeneous and irradiated porous membranes and their composite membrane. (Irradiated membrane side was exposed to lower pressure.) ○: observed values of homogeneous membrane; ●: values of irradiated porous membrane; ■: values of composite membrane; d_1 (homogeneous layer) = 1.46 μm, and d_2 (irradiated porous layer) = 12.87 μm.

higher pressure side. As shown in Figure 12 the permeability coefficient of the composite membrane was observed to be even lower than the homogeneous membrane when the irradiated membrane was exposed to the lower pressure side. The reason for this effect is not clear.

References

1. J. M. Thorman, H. Rhim, and S. T. Hwang, *Ch. Eng. Sci.*, **30**, 751 (1975).
2. S. A. Stern, T. F. Sinclair, P. J. Gareis, N. P. Vahldieck, and P. H. Mohr, *I & EC*, **57**, 49 (1965).
3. W. R. Vieth and J. A. Eilenberg, *J. Appl. Polym. Sci.*, **16**, 945 (1972).
4. H. K. Lonsdale, *J. Memb. Sci.*, **10**, 81 (1982).
5. T. Yamaji, *Kobunshi* (High Polymers, Japan), **30**, 187 (1981).
6. T. Nohmi, S. Manabe, K. Kamide, and T. Kaiwai, *Kobunshi Ronbunshu*, **34**, 729 (1977).
7. T. Nohmi, S. Manabe, K. Kamide, and T. Kaiwai, *Kobunshi Ronbunshu*, **34**, 737 (1977).
8. T. Nohmi, H. Makino, S. Manabe, K. Kamide, and T. Kaiwai, *Kobunshi Robunshu*, **35**, 253 (1978).
9. T. Nohmi, S. Manabe, K. Kamide, and T. Kawai, *Kobundhi Ronbunshu*, **35**, 509 (1978).
10. K. Kamide, S. Manabe, H. Mahino, T. Nohmi, H. Navila, and T. Kawai, *Polymer J.*, **15**, 179 (1983).
11. H. Fujita, *Chem. Eng.* (Japan), **25**, 74 (1961).
12. D. D. Fitts, *Nonequilibrium Thermodynamics*, McGraw Hill, New York, (1962).
13. F. J. Norton, *J. Appl. Polym. Sci.*, **1**, 1649 (1963).
14. J. A. Barrie, J. D. Levine, A. S. Michaels, and P. Wong, *Trans, Faraday Soc.*, **59**, 869 (1963).

Received March 7, 1985
Accepted February 17, 1986